Respiratory Research

RESEARCH

Open Access

Increased autophagy activity regulated by *LC3B* gene promoter DNA methylation is associated with progression to active pulmonary tuberculosis disease

Yung-Che Chen[1,2,3*†], Ying-Tang Fang[1†], Chao-Chien Wu[1], Tung-Ying Chao[1], Yi-Hsi Wang[1], Chia-Cheng Tseng[1], Sum-Yee Leung[1], Chiu-Ping Lee[1], Ting-Ya Wang[1], Po-Yuan Hsu[1], Jen-Chieh Chang[4], Meng-Chih Lin[1,3*] and Chang-Chun Hsiao[1,2*]

Abstract

Background This study aims to explore the role of autophagy-associated genes (ATG) and their epigenetic markers in the progression of *mycobacterium tuberculosis* (*M. tb*) infection, and to test the effects of de-methylation agents on macrophage functions against TB.

Methods ATG expressions and their gene promoter DNA methylation levels of blood immune cells were measured in 60 patients with active pulmonary TB disease, 31 subjects with latent TB infection (LTBI), and 15 non-infected healthy subjects (NIHS). An in vitro monocytic THP-1 cell culture model under *M. tb*-specific antigen stimuli was applied.

Results LC3B protein expression of blood M1/M2a monocyte, ATG5 protein expression of M2a, and mean DNA methylation levels of the *LC3B* gene promoter region of peripheral blood mononuclear cells were all increased in active TB patients versus either LTBI or NIHS group. The *LC3B* methylation levels were negatively correlated with its protein expressions. The discrimination of active TB disease from LTBI or NIHS was optimally captured by prediction scores, which combined LC3B (+) percentage of blood M1/M2a monocyte, *LC3B* gene promoter DNA methylation level, male gender, and body mass index. LC3B and ATG5 expressions of both blood M2a and neutrophil were decreased after 6-month anti-TB therapy, but hypermethylated *LC3B* gene promoter persisted. In vitro 5-Aza-

†Yung-Che Chen and Ying-Tang Fang contributed equally to this work.

*Correspondence:
Yung-Che Chen
yungchechen@yahoo.com.tw
Meng-Chih Lin
linmengchih@hotmail.com
Chang-Chun Hsiao
cchsiao@mail.cgu.edu.tw

Full list of author information is available at the end of the article

2′-deoxycytidine treatment improved bactericidal, apoptosis and phagocytosis functions through augmenting autophagy flux via mechanisms other than demethylation of the *LC3B* gene promoter in THP-1 cells.

Conclusions Increased LC3B expression and *LC3B* gene promoter hypermethylation may serve as biomarkers for progression of *M. tb* infection, while use of de-methylation agent may be a potential approach to host-directed immunotherapy in active TB disease.

Keywords Pulmonary tuberculosis, Latent TB infection, Autophagy, LC3B, ATG5, p62, DNA methylation

Background

Tuberculosis (TB) remains the leading cause of death from a single infectious agent, causing almost twice as many deaths as acquired immune deficiency syndrome [1]. Worldwide, an estimated 10.6 million people developed TB and an estimated 410,000 people developed multidrug-resistant or rifampicin-resistant TB in 2022, while the total number of deaths caused by TB was 1.3 million [2, 3]. Current challenges in TB include low disease detection rate, lack of robust markers indicating progression from latent TB infection (LTBI) to active TB, and increasing number of 'treatment-refractory' TB cases. Innovative insights into targeted immune modulation could drive new diagnostic or treatment strategies for ending the global TB epidemic [4].

Autophagy is a process in which cytosol and organelles are sequestered within double-membrane vesicles that deliver the contents to the lysosome/vacuole for degradation and recycling. Autophagy activation is critical for the regulation of innate immunity, inflammation, and antibacterial defenses [5]. Non-canonical autophagy includes selective autophagy targeting macromolecules and intracellular microbes (xenophagy), and microtubule associated protein 1 light chain 3 (MAP1LC3; LC3)-associated phagocytosis [6]. During *mycobacterium tuberculosis* (*M. tb*) infection, xenophagy is triggered via a reactive oxygen species (ROS)-dependent pathway. Then, the recognition of mycobacteria allows for forming ubiquitin chains, which recruit autophagy adaptors, such as SQSTM1 (p62), and link to LC3 of the autophagosomal membranes [7]. *M.tb*-triggered phagocytosis is a lipidated LC3B-conjugation process onto the single-membrane phagosome, during which autophagy related genes (ATG) 3/5/7/12/16L are recruited [7, 8]. *M. tb*-induced epigenetic modifications, such as DNA methylation, play an essential role in altering autophagy defense machanism [9]' [10]. In the mammalian genome, DNA methylation mostly occurs on 5-position of cytosine in the context of Cytosine-phosphate-Guanine (CpG) sequence, while DNA hypermethylation in gene promoters can cause decreased transcription of the downstream genes. Promoter regions of the *ATG5* and *LC3B* genes have been to shown to be hypermethylated accompanied by decreased gene expressions in macrophages from aged mice, while high-fat and high-fructose diet supplementation-induced autophagy impairment and M1 polarization can be reversed by reducing hypermethylation at the promotor regions of the *LC3B*, *ATG5*, and *ATG7* genes [11, 12]. It has yet been determined whether ATG expressions and their gene promoter DNA methylation statuses are associated with active TB disease [9].

In this study, we hypothesized that autophagy flux and DNA methylation levels of three core ATG gene promoters (*LC3B*, *ATG5*, *p62*) of blood immune cells may be different between active pulmonary TB patients, LTBI subjects, and non-infected healthy subjects (NIHS). Additionally, autophagy flux and epigenetic change of human monocytic THP-1 cells may be responsible for bactericidal and phagocytosis functions of macrophage, which may be improved with epigenetic drugs.

Methods

Study subjects

This study was conducted at Kaohsiung Chang-Gung Memorial Hospital in Taiwan from August 2020 to July 2023 in accordance with the Declaration of Helsinki. The Chang Gung memorial hospital's institutional review board approved the study protocol (certificate number: 201901817B0), and all subjects provided informed written consents before blood sampling. Gender of the participants was defined based on self-report. The specific criteria of enrollment for active TB were symptoms suggestive of active TB, and sputum collected for smear microscopy and mycobacterial culture showed at least one positive *M. tb* yielding on three separate occasions. All patients with active TB received standard anti-TB microbial agent treatment in a direct observed short-course manner. LTBI and NIHS groups included subjects with normal chest radiographic results and a lack of clinical symptoms suggestive of active TB, and classified based on blood interferon-γ releasing assay (IGRA) test positive and negative at 3rd month after close contact with the index open TB case, respectively. Patients with acquired immune deficiency syndrome, immunosuppressive disease, uncontrolled cancer with metastasis, and other active infections were excluded.

Processing of sputum samples for smear grading and mycobacterial culture

Sputum smears were done for acid fast bacilli (AFB), using both the Ziel-Nielsen stain and auramine-rhodamine stain. Smear grading was assessed by the World Health Organization scale. Sputum culture was done using both solid (LJ) and liquid (MGIT) media following standard procedures.

CXR grading of active pulmonary TB disease

The extent of radiographic lesion was graded based on the U.S. National Tuberculosis and Respiratory Disease Association scheme that classified disease into minimal, moderately advanced, and far-advanced disease. A far-advanced lesion was defined as slight-to-moderate density that extended more than the total volume of one lung or an equivalent in both lungs; total diameter of cavitation > 4 cm.

IGRA test by QuantiFERON-TB gold

The QFT-G assay (Cellestis Limited, Carnegie, Victoria, Australia) was used to assess interferon-gamma (IFN-γ) concentration on early secretory antigenic target-6 (ESAT-6), 10-kDa culture filtrate protein, mitogen (phytohemagglutinin, as a positive control), and a nil tube (as a negative control) by ELISA. The results were reported based on a borderline range recommended by the manufacturer, where a difference of ≥ 0.35 IU/ml between the level of IFN-γ measured in the TB antigen-exposed sample minus the level in the nil tube was considered positive.

Measurements of autophagy flux in peripheral blood immune cells (CD16+pneutrophil, CD14+CD209−M1 monocyte, CD14+CD209+M2a monocyte, CD3+CD4+ helper T cell, CD3+CD8+ cytotoxic T cell) by flowcytometry

Twenty milliliters venous blood was withdrawn from all study participants. To characterize the immune cell architecture, a panel consisting of unstained cells, isotype control (mouse IgG conjugated to (fluorescein isothiocyanate (FITC) and phycoerythrin (PE)), monocyte marker (CD14-PE-CyTM7), M2a marker (CD209-PerCP-Cy5.5), neutrophil marker (CD16-PC5), and helper/cytotoxic T cells marker (CD3- PE-CyTM5; CD4-PC7; CD8-PE-CyTM7; BD Pharmingen, USA) were chosen. To measure ATG5, LC3B, and p62 protein expressions separately, Alexa Fluor®488 anti-ATG5, anti-LC3B, and biotin anti-p62 plus PE streptavidin (eBioscience, USA) were used. For each test to be performed, 2 mL of fresh heparinized whole blood was lysed with OptiLyse C Lysis solution (Beckman Coulter, France), then incubated with indicated antibodies for 15 min, and subsequently detected for autophagy flux expressions with 1×10^5 events gated in a side scatter versus frontal scatter plot by using CytomicsTM FC500 flow cytometer (Beckman Coulter, USA). Data were presented as mean fluorescence intensity (MFI), corrected for background fluorescence with the corresponding isotype controls, or percentage of positivity. Representative histograms of LC3B, ATG5, and p62 protein expressions in vivo and in vitro are presented in supplementary Fig. S1.

Measuring CpG-site-specific DNA methylation levels by bisulfite pyro-sequencing method

Peripheral blood mononuclear cells (PBMCs) were isolated from heparinized blood by using a two-layer Ficoll-Histopaque density gradient centrifugation (Histopaque 1.077 and 1.119; Sigma Diagnostics, USA) method. Genomic DNAs were extracted from PBMCs using a DNA extraction kit (Zymo Research, USA). Specific CpG sites in eight promoter regions of the *LC3B*, *ATG5*, and *p62* genes were assessed by bisulfite-pyrosequencing based on reference sequence information from NCBI (*LC3B*: NM_022818.5; *ATG5*: NM_004849.4; *p62*: NM_003933.5). Polymerase chain reaction (PCR) amplification primers and sequencing primers were designed by PyroMark Assay Design Software 2.0, and are listed in supplementary Table S1. Bisulfite treatment and PCR amplification were performed by means of the EpiTect 96 Bisulfite Kit (Qiagen, Hilden, Germany) and the PyroMark PCR kit (Qiagen), respectively, following the manufacturer recommendations. The PCR conditions were 45 cycles of 95 °C for 20 s, 50 °C for 20 s, and 72 °C for 20 s, followed by 72 °C for 5 min. Pyrosequencing reactions and cytosine methylation quantification were performed in a PyroMark Q24 system (Qiagen). Representative pyrograms of CpG di-nucleotides assayed of the *LC3B*, *ATG5*, and *p62* genes in vivo and in vitro are presented in supplementary Fig. S2, S3, S4, and S5.

In vitro monocyte cell lines culture under TB antigen stimuli

THP-1 monocytes were cultured ($1–4 \times 10^6$ cells/mL) in RPMI 1640 medium, and stimulated with pre-specified concentrations of the recombinant proteins for 1, 3, or 9 days: 1 μg /mL for ESAT6, antigen 85 A (Ag85A), or whole γ-irradiated *M.tb* dead cell (H37Rv) (all from BEI Resources, Manassas, USA; Biosafety Level I). For epigenetic drug experiments, cells were pre-treated with various concentrations of compounds (5-aza-2′-de-oxycytidine, 5-AZA, 1 or 10 μM; rapamycin, Rap, 100 nM or 500 nM) for 24 h, followed by 1 μg/ml ESAT6 stimuli for 24 h. All experiments were performed in triplicate, independently. Autophagy flux (LC3B, ATG5, p62) was analyzed using the flow cytometer as mentioned above.

Measurement of THP-1 intracellular ROS production for bactericidal activity

For observing intracellular ROS production, 3×10^6 THP-1 cells were treated with 10 mM 2',7'-dichlorodihydrofluorescein diacetate (H2DCFDA; catalog no. D6883, Sigma Aldrich). Staining was quantified by using a FACScan flow cytometry system (Becton Dickinson, USA), with the 488 nm laser for excitation and 535 nm for detection.

Measurement of cell apoptosis by flow cytometry analysis

Apoptosis was detected by flow cytometry with an Annexin V/Propidium iodide (PI) apoptosis detection kit (BD Biosciences, USA). THP-1 cells and dyes were incubated in the dark for 15 min. The cells were then assessed by flow cytometry FACScan (Becton Dickinson, USA).

Measurement of THP-1 cell viability by WST-1

WST-1 reagent (Roche, Mannheim, Germany) diluted 1:10 in growth medium was added into THP-1 cells grown in a 96-well plate (10^4 cells / well). The amount of viable cells was determined via *optical density* measurement using a microplate reader at 450 nm, with 600 nm as a reference wavelength.

Measuring phagocytosis index of macrophage by flowcytometry

THP-1 cells were differentiated into macrophages by treatment with 30 ng/mL phorbol-12-myristate 13-acetate (PMA, Sigma-Aldrich, Saint Luis, MO, USA) for 3 days. THP-1 macrophage (1×10^5 cells/mL) was then treated with 5-AZA (10μM) or Rap 100nM/500 nM for 24 h, followed by phosphate-buffered saline or ESAT6 (1 ug/ml) for 72 h. EAST-6 (1ug/ml) was incubated with specific antibody (EAST-6, Abcam, Cambridge, USA) for 15 min, followed by dye (CF488A, Sigma-Aldrich, Saint Luis, MO, USA) for 15 min. Then, the mix compounds (ESAT6-antibody-CF488A) were incubated with THP-1 macrophage (1×10^5 cells/ml) for 30 min, and assessed by using the CytomicsTM FC500 (Beckman Coulter; California, USA). Phagocytosis index was calculated using the percentage of ESAT6-CF488A (+) macrophages for three independent experiments.

Statistical analysis

Continuous variables were presented as the mean ± standard deviation. ANOVA, Kruskal-Wallis H, chi-square, and paired t tests were used to assess the differences between groups where appropriate. Linear regression analysis with age, sex, body mass index (BMI), history of smoking/alcoholism, and co-morbidities entered in a single step was used to adjust *p* values in the comparisons of continuous values. Independent factors associated with active TB disease were combined in a mathematical formula based on binary logistic regression analysis, creating a prediction score. To assess diagnostic accuracy, the candidate biomarker was analyzed by area under the receiver operating characteristic (ROC) curves (AUC). Pearson correlation coefficient was used to measure the linear correlation between two continuous variables. All tests are two tailed and the null hypothesis is rejected at $p < 0.05$. A statistical software package (SPSS, version 22.0, SPSS Inc., Chicago, IL) was used for all analyses.

Results

Demographics of the study participants

A total of 106 subjects were enrolled and divided into three groups: 60 active TB patients, 31 LTBI subjects, and 15 NIHS. Baseline characteristics are presented in Table 1. Gender, comorbidities, alcoholism, and smoking history of the study participants were not significantly different between the three groups. Patients with active pulmonary TB disease had a lower BMI and a higher proportion of male gender compared with either NIHS or LTBI group.

Increased LC3B and ATG5 protein expressions of M1/M2a monocytes in active TB patients vs. either LTBI or NIHS group

LC3B (+) percentage of blood $CD14^+CD209^-$M1 monocyte was increased in active TB (51.98% ± 35.97%) versus NIHS group (15.8% ± 24.8%, $p = 0.001$) or LTBI group (25.6% ± 28.6%, $p = 0.003$, Fig. 1A). Similarly, LC3B (+) percentage of blood $CD14^+CD209^+$M2a monocyte was increased in active TB patients (69.6 ± 42.4%) versus NIHS (16.5 ± 29.1%, $p < 0.001$) or LTBI subjects (31.5 ± 40.9%, $p < 0.001$, Fig. 1B). Additionally, ATG5 (+) percentage of blood M2a monocyte was increased in active TB (63.0 ± 41.2%) versus NIHS (30.7 ± 36.3%, $p = 0.026$) or LTBI group (43.8 ± 42.4%, $p = 0.038$, Fig. 1C).

Increased LC3B, ATG5, and p62 protein expressions in active TB patients with high bacterial burden or far-advanced lesion on CXR versus those without specific characteristic or NIHS plus LTBI group

LC3B (+) percentage of blood $CD3^+CD8^+$cytotoxic T cell was increased in active TB patients with high bacterial burden (AFB 3 + or 4+; $n = 13$; 40.2 ± 40.3%) versus those with low bacterial burden (AFB 0, 1 + or 2+; $n = 47$; 13.1 ± 20.1%, $p < 0.001$) or NIHS plus LTBI group ($n = 46$; 13.0 ± 17.3%, $p = 0.005$, Fig. 1D). ATG5 (+) percentage of cytotoxic T cell was increased in active TB patients with high bacterial burden (41.3 ± 43.6%) versus those with low bacterial burden (13.1 ± 20.3%, $p < 0.001$) or NIHS plus LTBI group (16.8 ± 20.1%, $p = 0.009$, Fig. 1E). P62 protein expression of M2a monocyte was increased in active TB patients with far-advanced lesion on CXR ($n = 25$; 4.7 ± 7.8 MFI) versus either those with minimal

Table 1 Demographic and baseline characteristics of all the 106 study participants

	Non-infected healthy subjects *N* = 15	Subjects with latent TB infection *N* = 31	Patients with active pulmonary TB disease *N* = 60	*P* value
Age, years	52.8 ± 17.1	56.3 ± 16.7	59.8 ± 14.3	0.243
Male sex, n (%)	5 (33.3)	11 (35.5)	36 (60)	0.036
BMI, kg/m2	24.9 ± 5.4	24.9 ± 4.2	22.3 ± 3.7	0.01
Co-morbidity, n (%)				
Hypertension	2 (13.3)	7 (22.6)	12 (20)	0.761
Diabetes mellitus	2 (13.3)	9 (29)	11 (18.3)	0.366
Chronic obstructive pulmonary disease	0 (0)	1 (3.2)	4 (6.7)	0.496
Chronic hepatitis	4 (26.7)	3 (9.7)	6 (10)	0.185
Chronic kidney disease	2 (13.3)	1 (3.2)	5 (8.3)	0.449
Heart disease	0 (0)	3 (9.7)	1 (1.7)	0.117
Alcoholism, n (%)	2 (13.3)	2 (6.5)	9 (15)	0.54
Smoking				0.16
Current smoker, n (%)	1 (6.7)	8 (25.8)	16 (26.7)	
Former smoker, n (%)	2 (13.3)	3 (9.7)	14 (23.3)	
IGRA (+), n (%)	0 (0)	31 (100)	NA	
Acid fast bacilli 3 + or 4+, n (%)			13 (21.7)	
Drug-resistant TB, n (%)			8 (13.3)	
Systemic symptoms, n (%)			35 (58.3)	
Far advanced lesion on CXR, n (%)			25 (41.7)	

or moderately advanced lesion on CXR ($n = 35$; 1.6 ± 1.5 MFI, $p = 0.016$) or NIHS plus LTBI group ($n = 46$; 2.4 ± 2.3 MFI, $p = 0.031$, Fig. 1F).

Reduced LC3B/ATG5 expressions of blood CD14+CD209+M2a monocyte and LC3B/ATG5 expressions of blood CD16+ neutrophil after anti-TB treatment

In 30 active TB patients whose blood samples were obtained again after 6-month anti-TB therapy, both LC3B (+) percentage of M2a monocyte (41.1 ± 48.3% vs. 71.2 ± 41.1%, $p = 0.015$, Fig. 2A) and ATG5 (+) percentage of M2a monocyte (33.9 ± 46.4% vs. 68.0 ± 40.1%, $p = 0.006$, Fig. 2B) were reduced to near normal range (NIHS plus LTBI group; M2a LC3B: 41.1 ± 48.3% vs. 27.1 ± 38.1%, $p = 0.474$; M2a ATG5: 33.9 ± 46.4% vs. 42.2 ± 41.5%, $p = 0.253$) after treatment as compared with that at diagnosis, while both LC3B (+) percentage of neutrophil (22.1 ± 23.4% vs. 39.2 ± 31.1%, $p = 0.005$; Fig. 2C) and ATG5 (+) percentage of neutrophil (13.1 ± 19.2 vs. 38.8 ± 37.2, $p < 0.001$, Fig. 2D) were decreased significantly as compared with either that at diagnosis or with that in NIHS plus LTBI group (neutrophil LC3B: 22.1 ± 23.4% vs. 35.9 ± 38.1%, $p = 0.042$; neutrophil ATG5: 34.6 ± 39.1% vs. 38.8 ± 37.2, $p = 0.006$).

Hypermethylated *LC3B* gene promoter region in active TB patients versus LTBI subjects or NIHS

Mean DNA methylation levels over − 172, − 157, − 153, − 141, − 134, and − 118 CpG sites of the *LC3B* gene promoter region were increased in active TB patients (5.42 ± 2.34%) versus either LTBI subjects (3.98 ± 1.23%, $p = 0.005$) or NIHS group (4.08 ± 1.29%, $p = 0.039$, Fig. 3A), and negatively correlated with LC3B protein expressions of both blood M2a (R=-0.267, $p = 0.004$, Fig. 3B) and M1 (R=-0.193, $p = 0.04$) monocytes. In the 30 active TB patients whose blood samples were obtained again after 6-month anti-TB treatment, the *LC3B* promoter DNA methylation status showed no significant difference after treatment as compared with that at diagnosis (5.18 ± 2.35% versus 5.3 ± 2.4%, $p = 0.774$, Fig. 2E) and remained elevated as compared with that in NIHS plus LTBI group (5.18 ± 2.35% versus 4.09 ± 1.35%, $p = 0.023$). DNA methylation levels of the *ATG5*, and *p62* gene promoters were not different between the three groups.

An optimal discrimination of active pulmonary TB disease from LTBI and NIHS by prediction score 1 and 2, respectively

Stepwise multivariate logistic regression analysis using all the parameters at diagnosis that showed statistical difference between active TB and LTBI groups revealed that LC3B (+) percentage of M2a (OR 1.029, 95% CI1.013–1.044, $p < 0.001$), mean DNA methylation level of the *LCB3* gene promoter region (OR 1.998, 95% CI 1.295–3.082, $p = 0.002$), BMI (OR 0.649, 95% CI 0.511–0.824, $p < 0.001$) and male gender (OR 6.437, 95% CI 1.11-37.318, $p = 0.038$) were independent factors for discrimination between active TB and LTBI. To increase

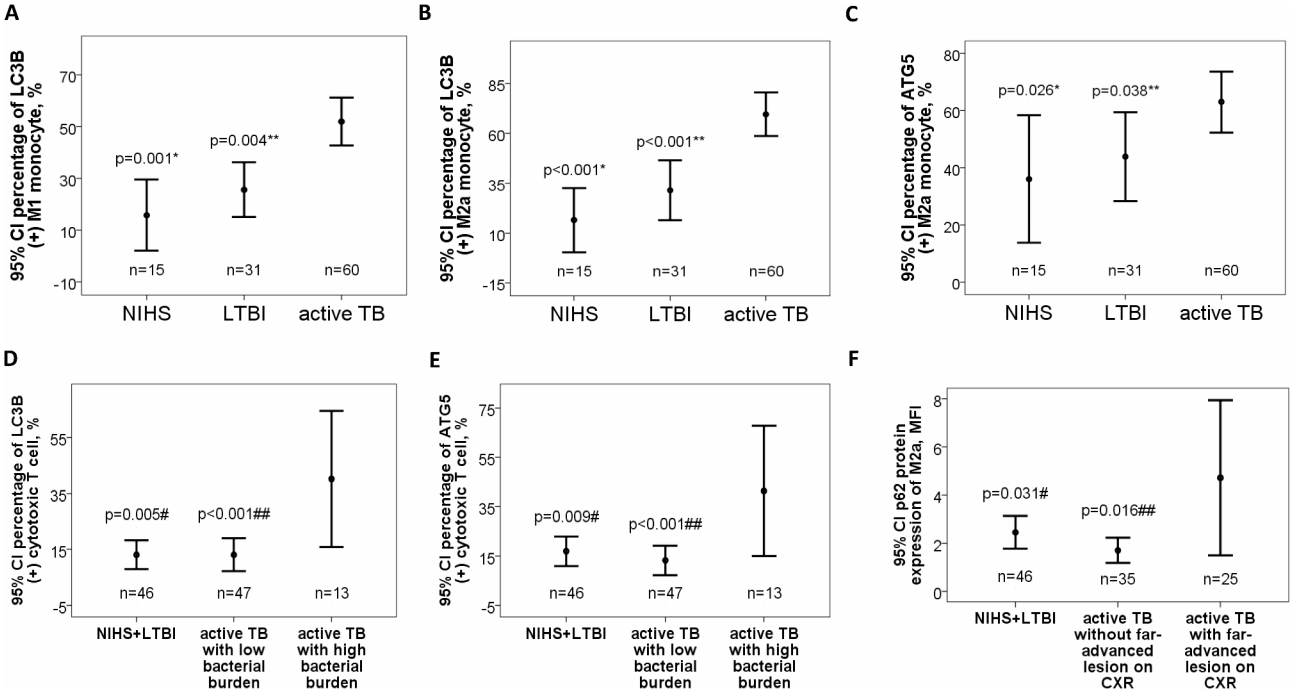

Fig. 1 Increased autophagy flux of blood immune cells in patients with active pulmonary TB disease. By using flowcytometry method, 1×10^5 events were collected with blood immune cells gated in a side scatter versus frontal scatter plot to identify monocytes. Monocytes were then analyzed for expressions of CD14 and CD209 in the FL1 and Fl2 channels, respectively, using a dual staining protocol to identify M1 ($CD14^+CD209^-$) and M2a ($CD14^+CD209^+$). These two groups of monocytes were further analyzed for protein expressions of ATG5, LC3B, and p62. (**A**) LC3B (+) percentage of blood $CD14^+CD209^-$ M1 monocyte was increased in active TB versus either latent TB infection (LTBI) or non-infected healthy subject (NIHS) group. (**B**) LC3B (+) percentage of blood $CD14^+CD209^+$ M2a monocyte was also increased in active TB versus either LTBI or NIHS group. (**C**) ATG5 (+) percentage of blood $CD14^+CD209^+$ M2a monocyte was increased in active TB versus either NIHS or LTBI group. (**D**) LC3B (+) percentage, and (**E**) ATG5 (+) percentage of blood $CD3^+CD8^+$ cytotoxic T cells were both increased in active TB patients with high bacterial burden versus either those with low bacterial burden or NIHS plus LTBI group. (**F**) P62 protein expression of blood M2a monocyte was increased in active TB patients with far-advanced lesion on CXR versus either those with mild to moderate lesion on CXR or NIHS plus LTBI group

*compared between active TB and NIHS group, and adjusted by linear regression

**compared between active TB and LTBI group, and adjusted by linear regression

#compared between active TB patients with a specific phenotype and NIHS plus LTBI group

##compared between active TB patients with and without a specific phenotype

diagnostic accuracy, the four factors were combined in the model formula (Fig. 3C). The discrimination of active TB from LTBI was optimally captured by Prediction Score 1 (AUC = 0.883, 95% CI 0.812–0.955, $p < 0.001$) (Fig. 3D). Probability at a cutoff value of 0.663 displayed a sensitivity of 80.9% and specificity of 76.7%, dividing the patient population into high-risk and low-risk groups for progression from LTBI to active TB disease.

Stepwise multivariate logistic regression analysis using all the parameters that showed statistical difference between active TB and NIHS revealed that LC3B (+) percentage of M2a (OR 1.026, 95% CI 1.002–1.051, $p = 0.033$), LC3B (+) percentage of M1 (OR 1.049, 95% CI 1.004–1.095, $p = 0.033$), mean DNA methylation level of the *LCB3* gene promoter region (OR 2.305, 95% CI 1.218–4.364, $p = 0.01$), and BMI (OR 0.736, 95% CI 0.573–0.946, $p = 0.017$) were independent factors for discrimination between active TB and NIHS. To increase diagnostic accuracy, the four factors were combined in the model formula (Fig. 3E). The discrimination of active TB from NIHS was optimally captured by Prediction Score 2 (AUC = 0.929, 95% CI 0.852–1, $p < 0.001$) (Fig. 3F). Probability at a cutoff value of 0.609 displayed a sensitivity of 96.7% and specificity of 86.7%, dividing the patient population into high-risk and low-risk groups for progression from NIHS to active TB disease.

Increased DNA methylation levels of the *LC3B* and *ATG5* gene promoter regions in active TB patients with systemic symptoms

Subgroup analysis showed that DNA methylation level over −63 CpG site of the *LC3B* gene was increased in active TB patients with systemic symptom (fever or body weight loss, $n = 35$; $4.37 \pm 3.51\%$, Fig. 4A) as compared with that in those without systemic symptom ($n = 25$; $2.86 \pm 2.17\%$, $p = 0.03$) or NIHS plus LTBI group ($n = 46$; 3.14 ± 2.2, $p = 0.003$), and negatively correlated with LC3B protein expression of blood M2a monocyte (R=-0.199,

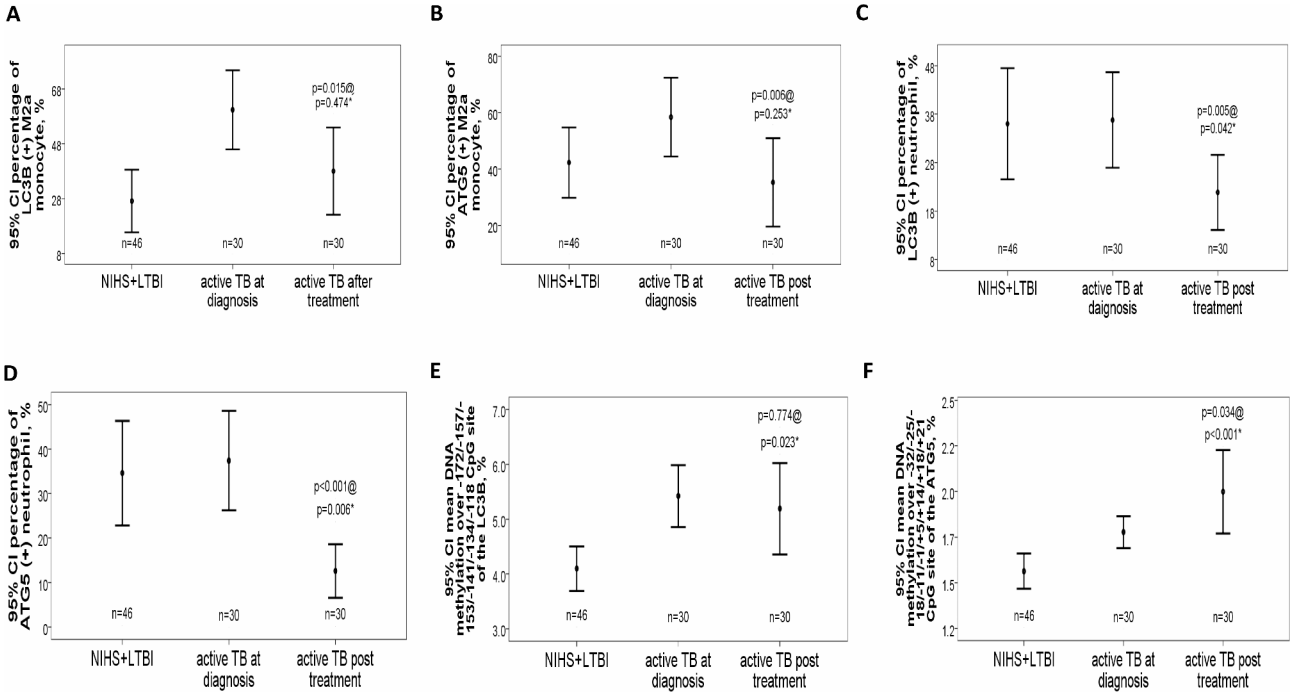

Fig. 2 Reduced autophagy flux and change in DNA methylation levels of blood immune cells in active TB patients after 6-month anti-TB treatment. In 30 active TB patients whose blood samples were collected again after 6-month anti-TB therapy, both (**A**) LC3B (+) percentage and (**B**) ATG5 (+) percentage of blood $CD14^{+}CD209^{+}$ M2a monocyte were reduced versus at diagnosis and not different from that in NIHS + LTBI group, while (**C**) LC3B (+) percentage and (**D**) ATG5 (+) percentage of blood $CD16^{+}$ neutrophil were reduced after treatment versus either at diagnosis or NIHS + LTBI group. (**E**) Mean DNA methylation levels over − 172, − 157, − 153, − 141, − 134, and − 118 CpG sites of the *LC3B* gene promoter region in active TB patients after treatment did not change significantly versus at diagnosis, and remained elevated versus NIHS + LTBI group. (**F**) Mean DNA methylation level over − 32, -25, -18, -11, -1, + 5, +14, + 18, and + 21 CpG sites of the *ATG5* gene in active TB patients after treatment were increased versus either at diagnosis or NIHS + LTBI group
@compared between active TB patients after and before 6-month anti-TB treatment
*compared active TB patients after 6-month anti-TB treatment with non-infected healthy subjects (NIHS) plus latent TB infection (LTBI) group

$p = 0.034$, Fig. 4B). Similarly, DNA methylation level over − 30 CpG site of the *LC3B* gene was increased in active TB patients with systemic symptom ($n = 35$; 6.25 ± 3.76%, Fig. 4C) as compared with that in those without systemic symptom ($n = 25$; 4.64 ± 2.06%, $p = 0.043$) or NIHS plus LTBI group ($n = 46$; 4.2 ± 2.3%, $p < 0.001$), and negatively correlated with LC3B protein expressions of helper T cell (R=-0.195, $p = 0.038$, Fig. 4D). Additionally, mean DNA methylation level over − 32, -25, -18, -11, -1, + 5, +14, + 18, and + 21 CpG sites of the *ATG5* gene was increased in active TB patients with (1.69 ± 0.37%, $p < 0.001$) and without systemic symptom (1.72 ± 0.34%, $p = 0.016$) as compared with that in NIHS plus LTBI group (1.52 ± 0.32%, Fig. 4E), and negatively correlated with ATG5 (+) percentage of helper T cell (R=-0.218, $p < 0.05$, Fig. 4F). In the 30 active TB patients whose blood samples were obtained again, DNA methylation levels of the three core ATG genes did not showed significant changes after 6-month anti-TB treatment, except that mean DNA methylation level over − 32, -25, -18, -11, -1, + 5, +14, + 18, and + 21 CpG sites of the *ATG5* gene was further increased after treatment (1.87 ± 0.57 versus 1.67 ± 0.33%, $p = 0.043$, Fig. 2F) and remains elevated as compared with that in NIHS + LTBI group (1.87 ± 5.7 versus 1.51 ± 0.32%, $p < 0.001$).

Enhanced autophagy flux in response to various TB-specific antigen stimuli in vitro

In THP-1 cells, both LC3B (+) and ATG5 (+) percentages were increased in response to ESAT-6, Ag85A and ESAT-6 + Ag85A co-stimuli versus for 24 h versus normal culture medium control (NC) (Fig. 5A and B). ROS production was increased in response to ESAT-6, Ag85A, and ESAT-6 plus Ag85A co-stimuli versus NC (Fig. 5C), and positively correlated with LC3B (+) percentage ($R = 0.762$, R square = 0.623, $p = 0.004$). Early apoptosis marker was increased in response to ESAT-6, Ag85A and ESAT-6 + Ag85A co-stimuli versus NC (Fig. 5D), and positively correlated with LC3B (+) percentage ($R = 0.822$, R square = 0.679, $p = 0.001$).

To determine midterm and long-term effects of different TB-specific antigens on autophagy flux and epigenetic change, we extended the incubation period to 3 and 9 days, respectively. In THP-1 cells, LC3B (+) percentage, ATG5 (+) percentage, and p62 (+) percentage were all increased in response to ESAT-6 after either 3-day or

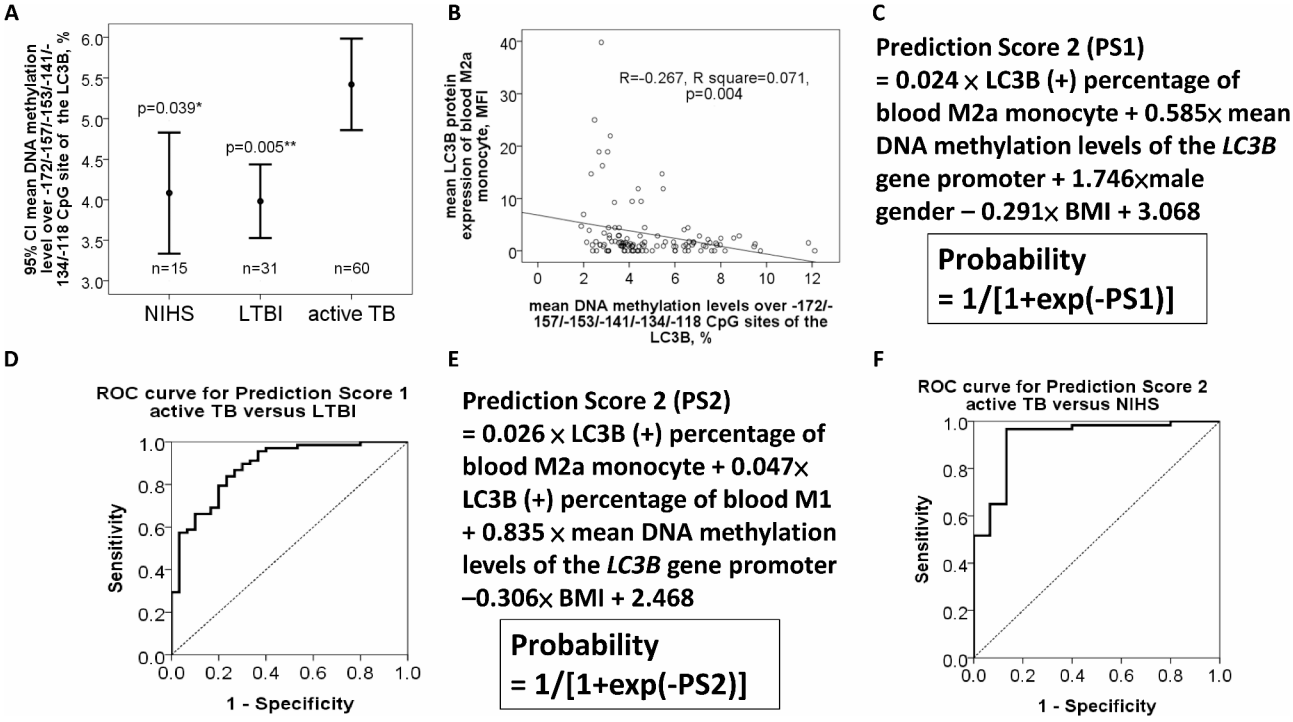

Fig. 3 Predictive accuracy of the *LC3B* gene promoter DNA methylation levels and Prediction Score 1/2 for active pulmonary TB. (**A**) Mean DNA methylation levels over – 172, -157, -153, -141, -134, and – 118 CpG sites of the *LC3B* gene promoter region were increased in active TB patients versus either NIHS or LTBI group, and negatively correlated with both (**B**) LC3B (+) percentage of blood M2a monocyte. (**C**) Using binary logistic regression analysis, the four independent factors for active TB versus LTBI could be combined in a model formula, resulting in a prediction score 1 (PS1). (**D**) The risk of progression from LTBI to active TB was optimally captured by the PS1. (**E**) Using binary logistic regression analysis, the four independent predictors for active TB versus NIHS could be combined in a model formula, resulting in a prediction score 2 (PS2). (**F**) The risk of progression from NIHS to active TB was optimally captured by the PS2

*compared between active TB and NIHS group, and adjusted by linear regression

**compared between active TB and LTBI group, and adjusted by linear regression

9-day stimuli versus NC. LC3B (+), ATG5 (+), and p62 (+) percentages were all increased in response to H37Rv after 3-day stimuli, but decreased after 9-day stimuli versus NC (Fig. 5E and G). Additionally, *LC3B* gene expression was increased with ESAT6 stimuli in the presence or absence of 5-AZA treatment (Fig. 5H).

De-methylation agent, 5-AZA, treatment resulted in improved autophagy flux, ROS production, late apoptosis, and phagocytosis in THP-1 cells stimulated with ESAT-6

To determine the effects of de-methylation agent and autophagy enhancer on bactericidal, apoptosis, phagocytosis, and autophagy functions, THP-1 cells were treated with either 5-AZA or Rap, followed by ESAT-6 stimuli for 3 days. 5-AZA treatment resulted in increased autophagy flux (percent of LC3B (+) cells, Fig. 6A; percent of ATG5 (+) cells, Fig. 6B; percent of p62 (+) cells, Fig. 6C; supplementary Fig. S1), increased ROS production (percent of H2DCFDA (+) cells, Fig. 6D), and increased late apoptosis (percent of PI (+) and annexin V (+) cells, Fig. 6E) in the presence or absence of ESAT-6 stimuli as compared with that in ESAT-6 alone or NC condition. On the other hand, high dose Rap treatment resulted in mild increase in autophagy flux only in the absence of ESAT-6 stimuli, while it increased late apoptosis but decreased ROS production in the presence of ESAT-6 stimuli. Finally, phagocytosis index of THP-1 macrophage (CF488A (+) percentage) at 30 min was increased with ESAT-6 stimuli, and further increased with either 5-AZA or low dose Rap treatment (Fig. 6F). Cell viability (WST-1 (+) THP-1 cell relative to normal control (NC)) was decreased to less than 70% with ESAT-6 alone stimuli, and increased to around 80% with either 5-AZA or Rap co-treatment (Fig. 6G). Mean DNA methylation level over – 172/-157/-153/-141/-134/-118 CpG sites of the *LC3B* gene was decreased with 5-AZA alone treatment vs. NC, but did not show significant change with either Rap alone, ESAT-6 alone, ESAT6 + 5-AZA, or ESAT6 + Rap treatment (Fig. 6H). Figure 7 depicts the proposed interplay between ROS-mediated autophagy-related genes and hypermethylated *LC3B* gene promoter epigenotype in the model of host-directed immunotherapy for *M. tb* infection.

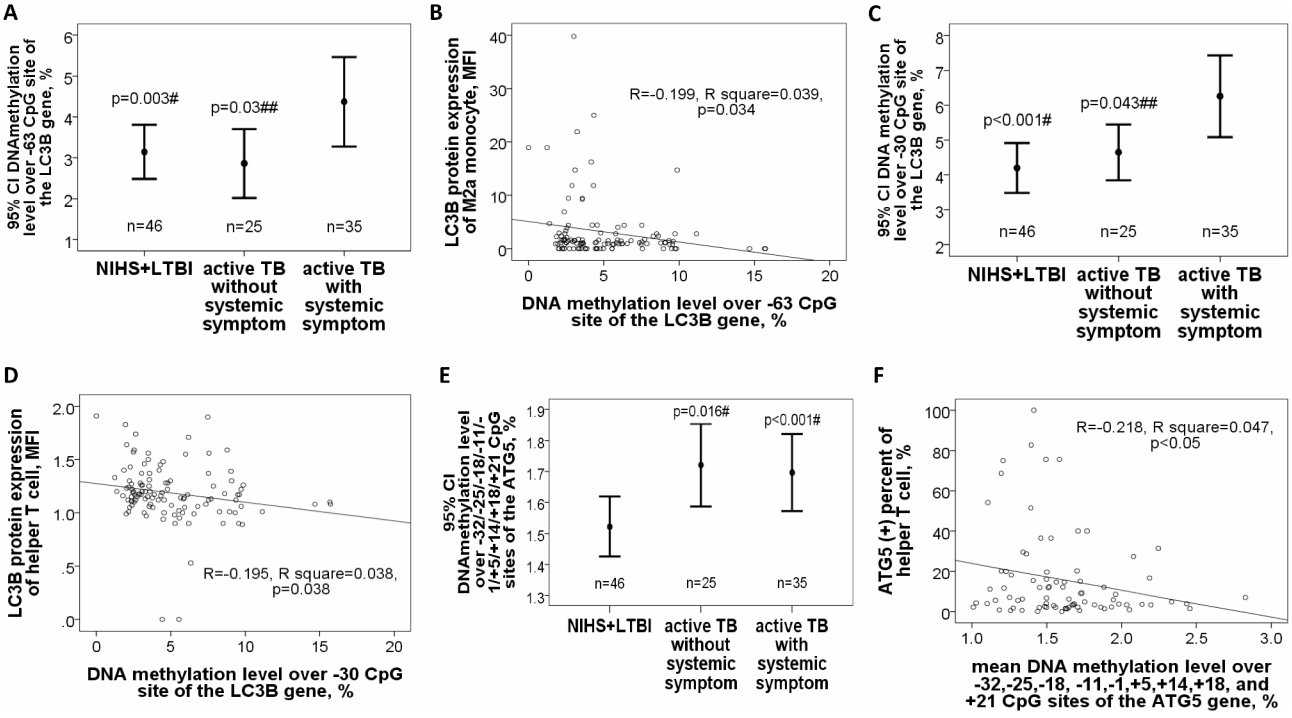

Fig. 4 Increased DNA methylation levels of the *LC3B* and *ATG5* gene promoter regions in active TB patients with systemic symptoms. DNA methylation levels over − 63 CpG site of the *LC3B* gene was (**A**) increased in active TB patients with systemic symptoms (fever, body weight loss, or both) as compared with that in those without systemic symptoms or NIHS plus LTBI group, and (**B**) negatively correlated with LC3B protein expression of blood M2a monocyte. DNA methylation levels over − 30 CpG site of the *LC3B* gene (**C**) increased in active TB patients with systemic symptoms (fever, body weight loss, or both) as compared with that in those without systemic symptoms or NIHS plus LTBI group, and (**D**) negatively correlated with LC3B protein expression of blood helper T cell. Mean DNA methylation level over − 32, -25, -18, -11, -1, + 5, +14, + 18, and + 21 CpG sites of the *ATG5* gene was (**E**) increased in active TB patients with or without systemic symptoms, and (**F**) negatively correlated with ATG5 (+) percentage of helper T cell

#$p < 0.05$, compared with NIHS + LTBI group

##$p < 0.05$, compared with active TB patients without systemic symptom

Discussion

Blood immune biomarkers that can early distinguish active TB disease from both LTBI and NIHS are still lacking. This study was undertaken to explore the roles of autophagy associated molecules and epigenetic markers in the progression from NIHS through LTBI to active pulmonary TB disease. Through measuring autophagy flux and epigenetic changes in blood immune cells, we found that increased LC3B protein expressions and *LC3B* gene promoter DNA methylation levels of blood immune cells independently distinguished active pulmonary TB disease from either LTBI or NIHS. Furthermore, we demonstrated that the de-methylation agent, 5-AZA, improved bactericidal, autophagy, apoptosis, and phagocytosis functions of macrophage in vitro through mechanisms other than demethylation of the *LC3B* gene promoter region.

Autophagy is often hijacked or manipulated by many pathogens [13–15]. *M. tb* can exploit virulence factors to effectively dampen host-directed autophagy utilizing diverse mechanisms, while host autophagy activation plays an essential role in the enhancement of antimicrobial immune responses and controlling pathological inflammation against *M. tb* [16]. Moreover, autophagy-regulated initiation of trained immunity contributes to the prevention of *M. tb* infection [17]. However, the roles of autophagy remain largely uncharacterized in the context of clinical biomarkers for early identification of progression from NIHS or LTBI to active TB disease. For the first time, we found that LC3B and ATG5 were both up-regulated in active TB patients, and further up-regulated in those with high bacterial burden or far-advanced disease, while reversed with anti-TB therapy. These findings suggest that autophagy flux may be used to develop monitoring tools for disease progression of TB re-activation. In line with our findings, it has been reported that M1-polarized macrophages show nitric oxide and autophagy-dependent degradation of *M. tb* in vitro, leading to increased antigen presentation to T cells through an ATG-RAB7-cathepsin pathway, while M2-polarized macrophages are permissive for *M. tb* proliferation through histone deacetylation-mediated autophagy impairment [18].

Another important finding in the current study was increased DNA methylation levels of the *LC3B* gene promoter region in active TB patients. Previous studies

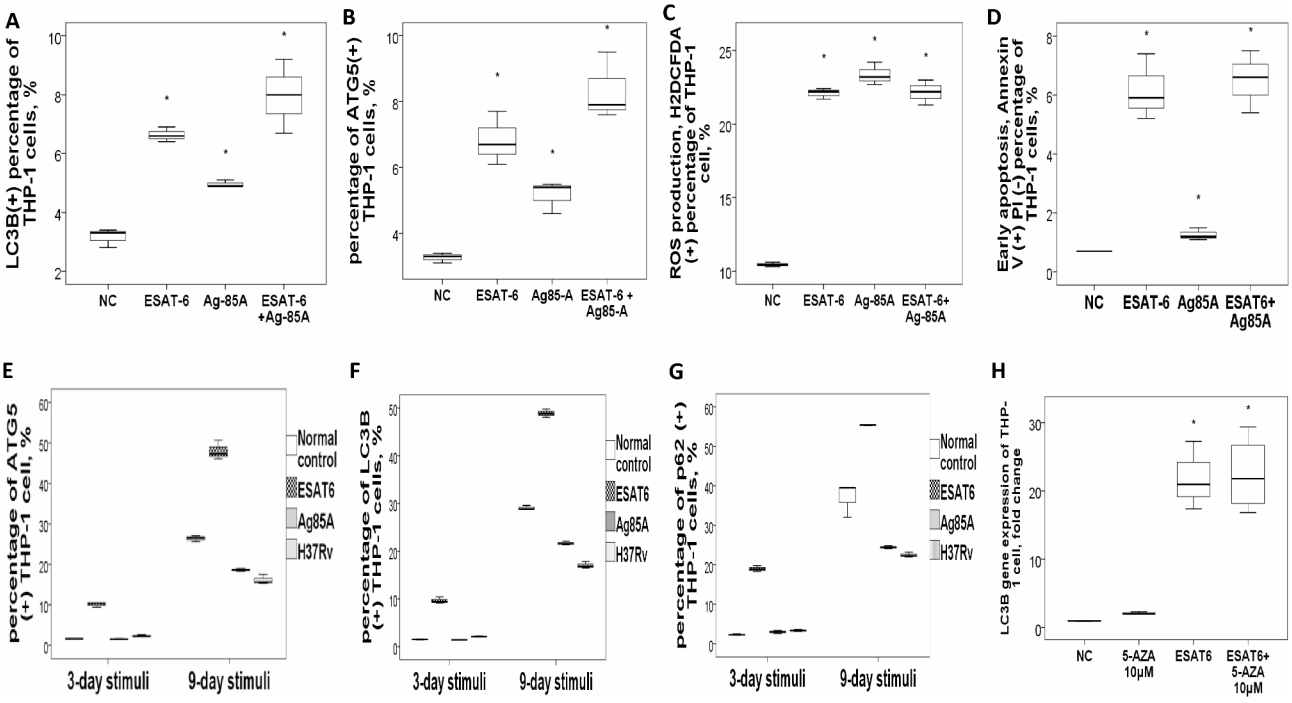

Fig. 5 Changes in autophagy flux of monocytic THP-1 cells in response to in vitro stimuli with *M. tb* specific antigens and γ-irradiated whole *M. tb* cell. (**A**) LC3B (+) percentage, (**B**) ATG5 (+) percentage, (**C**) production of reactive oxygen species (ROS), and (**D**) early apoptosis were all increased in THP-1 cells in response to ESAT-6, Ag85A, or both mixture stimuli for 24 h versus normal control (NC). Percentages of (**E**) LC3B (+), (**F**) ATG5 (+), and (**G**) p62 (+) THP-1 cells were all increased in response to ESAT-6 stimuli at either day 3 or day 9. Percentage of (**E**) LC3B (+), (**F**) ATG5 (+), and (**G**) p62 (+) THP-1 cells were not altered in response to Ag85A stimuli at day 3, but decreased at day 9. Percentage of (**E**) LC3B (+), (**F**) ATG5 (+), and (**G**) p62 (+) THP-1 cells were all increased in response to H37Rv stimuli at day 3, but decreased at day 9. (**H**) LC3B gene expression was increased with ESAT-6 stimuli in the presence of absence of 5-AZA treatment

*$p < 0.05$, compared with normal control (NC)

#$p < 0.05$, compared with ESAT-6 alone condition

have shown that *M. tb* triggers epigenetic modifications to manipulate autophagy for its survival benefits. For instance, host microRNA (miR)-30a, miR-155, and miR-1303 can inhibit *M. tb*-induced autophagy through targeting ATG3 and ATG2b [19]. It has been shown that *M. tb* provokes its survival in host cells through blocking autophagy by triggering hyper-methylation of histone H3 lysine 9 at the *Atg5* and *Atg7* gene promoter regions through activation of p38-MAPK- and EHMT2 methyltransferase-dependent signalling pathways [20]. Inherited DNA methylation patterns (epigenotype) may affect the susceptibility to specific infection, while chronic infection may suppress host immunity through DNA methylation changes. Our previous epigenome-wide study found that altered DNA methylation of the *miR-505*, *RPTOR*, and *WIPI2* genes may underlie autophagy-mediated immune responses to *M. tb*, and contribute to disease susceptibility [21]. Moreover, the promoter regions of the *ATG12* gene in cystic fibrosis macrophages are more methylated than in the wild-type immune cells, accompanied by low autophagy activity [22]. In the current study, we found increased DNA methylation levels of the *LC3B* promoter region in active TB patients as compared to that in either LTBI or NIHS, but were not reduced after anti-TB treatment. The in vitro experiments showed that neither *LC3B* or *ATG5* gene promoter methylation was altered with ESAT-6 stimuli, suggesting that hypermethylated *LC3B* gene promoter may be an epigenotype for susceptibility to active TB disease rather than an acquired change with chronic *M. tb* infection. Our finding provides a novel epigenetic mechanism underlying autophagy dysfunction in *M. tb* infection and re-activation. In line with our findings, a unique DNA methylation signature with no peripheral immune response to *M. tb* antigen has been demonstrated in individuals who later developed LTBI [23]. Moreover, global DNA methylation perturbations in active TB patients has been shown to persist 6 months after successful anti-TB treatment [24]. DNA methylation can also orchestrate other infectious circumstances through affecting autophagy flux. For instance, *Helicobacter pylori*-induced DNA hypermethylation has been reported to modulate LC3Av1suppression and autophagy flux impairment, resulting in elevated tumorigenicity of gastric epithelial cells [25]. Additionally, *Legionella* effector Lpg2936-induced 6 mA RNA hyper-methylation in the promoter region of the

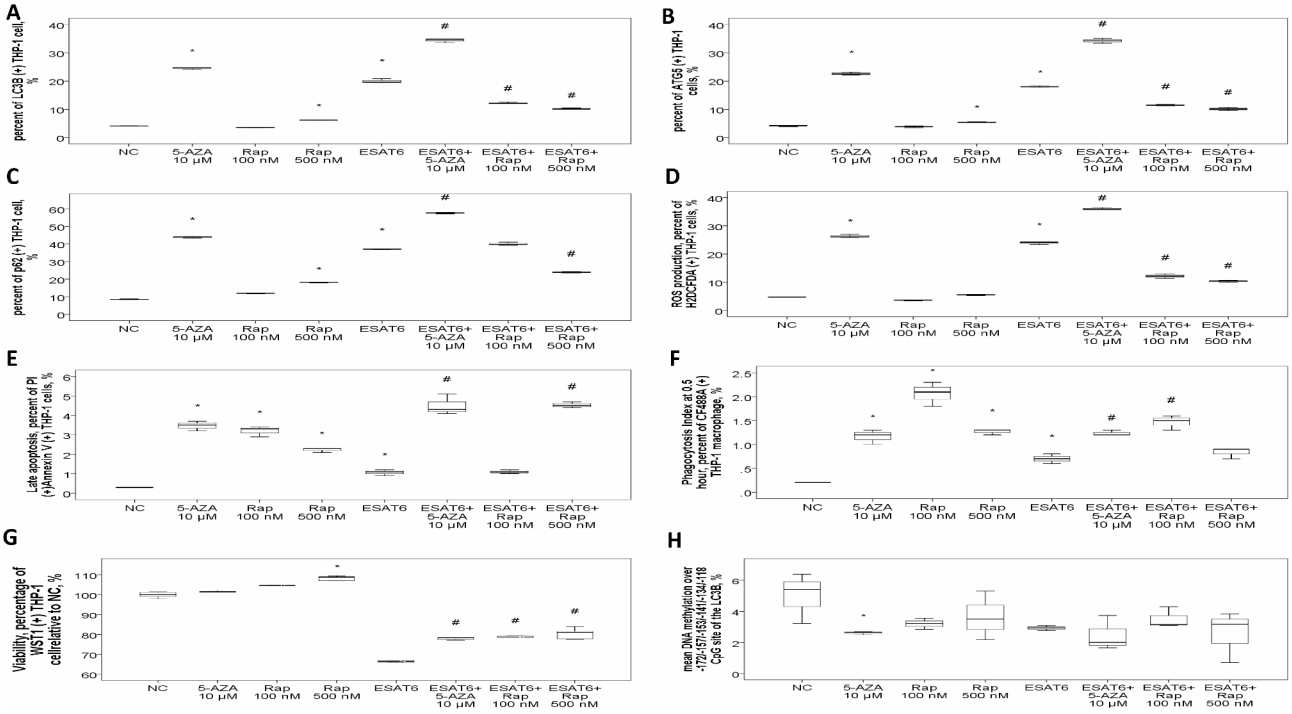

Fig. 6 Effects of 5-Aza-2′-deoxycytidine (5-AZA) treatment on autophagy flux, bactericidal, apoptosis, and phagocytosis functions in THP-1 cells. 5-AZA treatment resulted in further increase in autophagy flux, including (**A**) LC3B (+) percentage, (**B**) ATG5 (+) percentage, and (**C**) p62 (+) percentage in THP-1 cell stimulated with ESAT-6 as compared with that in ESAT-6 stimuli alone condition, while high dose rapamycin (Rap, an autophagy enhancer) treatment resulted in mild increase in autophagy flux only in the absence of ESAT-6 stimuli. 5-AZA treatment resulted in further increase in (**D**) reactive oxygen species (ROS; H2DCFDC (+) percentage) production and (**E**) late apoptosis (PI (+) and annexin V (+) percentage) in THP-1 cells stimulated with ESAT-6 as compared with that of ESAT-6 stimuli alone condition. (**F**) Both 5-AZA and low dose Rap treatment improved phagocytosis index (CF488A (+) percentage) of THP-1 macrophage measured at 30 min after co-culture with the ESAT-6-antibody-CF488A dye complex in the presence or absence of ESAT-6 stimuli. (**G**) Cell viability (WST-1 (+) percentage relative to normal control (NC)) was decreased with ESAT-6 stimuli, and increased to around 80% with either 5-AZA or Rap co-treatment. (**H**) Mean DNA methylation level over − 172/-157/-153/-141/-134/-118 CpG sites of the *LC3B* gene was decreased with 5-AZA alone treatment vs. NC, but did not show significant change in other conditions
*$p < 0.05$, compared with normal culture medium control (NC)
#$p < 0.05$, compared with ESAT-6 alone condition

Atg7 and *LC3B* genes accompanied by autophagy impairment can be restored with methylation inhibitors, 5-AZA and (2)-Epigallocatechin-3-gallate, resulting in disrupting bacterial replication in macrophage [26]. More investigations should be performed to determine the exact interplay between *LC3B* gene promoter hyper-methylation and autophagy flux in active TB disease.

Some immunological markers have been proposed for discrimination between LTBI and active TB. One example is the frequency of purified protein derivate-specific $CD4^+$ T cells only secreting TNF-α with an effector memory phenotype ($CD45RA^-CCR7^-CD127^-$) that distinguished active TB from LTBI [27]. Another is the T cellular and antibody response against *M. tb* dormancy survival regulator, DosR regulon-encoded antigens, that also distinguished active pulmonary TB from LTBI [28]. Several microRNAs, such as miR-889, miR223, miR-155, miR-150, miR146a, miR23, and miR-21, have shown some power to distinguish between LTBI and active TB [29]. Despite this progress, the search for a reliable biomarker for discriminating LTBI from active TB disease remains limited [30]. The current study is the first one linking autophagy activation of blood monocyte and epigenetic alteration of the *LC3B* gene promoter to TB reactivation. Combining LC3B (+) percentage of blood M1/2a monocyte, DNA methylation levels of the *LC3B* gene promoter and clinical factors (male, BMI), the Prediction Score 1 and 2 discriminated active TB patients from LTBI and NIHS, respectively, with good performance. In line with our findings, low BMI has been shown to be a significant risk factor for active TB disease, while data from epidemiology, humans, and animals suggest that males are more susceptible to active TB disease and associated with poorer outcomes than females [31–33]. Further large-scale studies are required to validate these findings.

Host-directed therapy is emerging as a novel concept to reduce the duration of antibacterial therapy or the amount of lung damage through improving immune defenses for active TB patients. Everolimus is an autophagy inducer through inhibiting mammalian target of

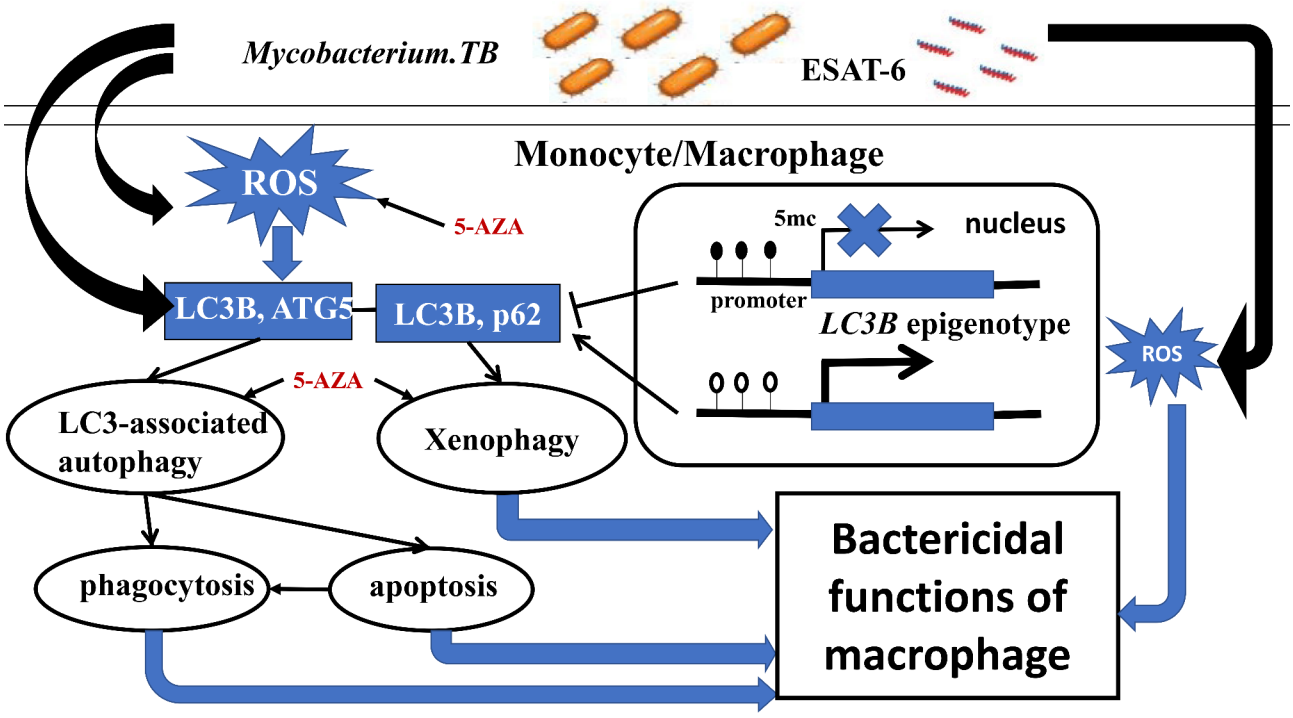

Fig. 7 The proposed interplay between autophagy-related genes and their epigenetic change in the model of host-directed immunotherapy for mycobacterium tuberculosis (*M. tb*) infection. A schematic diaphragm depicts the potential therapeutic effects of 5-azacytidine (5-AZA) on apoptosis, phagocytosis, and bactericidal functions of macrophage probably through augmenting production of reactive oxygen species (ROS) via demethylating reduction-oxygenation related genes. *M. tb* infection induces ROS-dependent LC3B-related phagocytosis and xenophagy, while DNA hypermethylation status of the *LC3B* gene promoter region (epigenotype) may contribute to progression to active TB disease by inadequate autophagy flux at confronting *M. tb* infection. 5-AZA may lead to improved autophagy, phagocytosis, and apoptosis functions of macrophage through inhibiting DNA methylation of reduction-oxygenation related genes or ATGs other than *LC3B*, *ATG5*, or *p62*. Arrows represent a positive action on the target, whereas bar-headed arrows represent an inhibition

rapamycin, and has been shown to decrease the viability of *M. tb* in the granulomas in vitro [34]. A phase 2 randomized open-label controlled trial showed that everolimus increased lung function parameter forced expiratory volume in one second (as a percentage of predicted) by 6.56% (about 200 ml) after 6-month concurrent anti-TB therapy in pulmonary cavitary TB patients, but did not affect sputum culture conversion rate [35]. About 5% of the *M. tb* genome encodes epigenetic modifiers that include kinases, methyltransferases, acetyltransferases, and succinyltransferases to counter host defense mechanisms for its proliferation. For instance, Rv2067c, Rv1515c, Rv1523, MamA, MamB, and HsdM are *M. tb*-secreted methyltransferases that can modulate host gene expressions of apoptosis, immune responses, redox, or drug targets and transporters [36–38]. On the other hand, altered methyltransferase and demethylase are another crucial mechanism modulating host immune responses against *M. tb* infection. For instance, G9a, SET8, and SUV39H1 are host histone methyltransferases that can regulate type I interferon response, oxidative stress and apoptosis functions, or directly reduce the cell adhesion capability of *M. tb* through tri-methylation of the mycobacterial histone-like protein, HupB [39–41]. In the current study, we demonstrated for the first time that 5-AZA, a DNA methyltransferase pan inhibitor, improved bactericidal, apoptosis, and phagocytosis functions of THP-1 cells stimulated with ESAT6, through augmentation of ROS-mediated autophagy flux but not through inhibiting DNA methylation of the *LC3B* or *ATG5* gene promoter region. In line with our findings, 5-AZA has been shown to deplete glutathione, leading to accumulation of ROS and/or mitochondrial superoxide in cancer cells [42, 43]. Further investigation is required to clarify underlying mechanisms and the role of DNA demethylation agents in host-directed therapy in active TB disease. The major drawback of DNA methyltransferase inhibitors is that they are unsuitable for precise targeting of a particular methylated CpG, are relatively non-specific with low chemical stability, and confer significant toxicities. Recently, the application of CRISPR/dCas9 in epigenetic editing makes it possible to modify individual DNA methylation at a defined gene region and regulate specific gene change with good specificity and efficiency [44]. Based on our results, epigenetic editing to modulate DNA methylation levels of the oxidation–reduction

related genes may be a promising approach to improving macrophage functions through augmenting autophagy flux during active *M. tb* infection.

There are several limitations that we should acknowledge in this study. First, the causal relationship between autophagy activation and ATG gene promoter methylation is not straightforward. Inherited DNA methylation aberrance (epigenotype) may affect autophagy activity and make individuals more susceptible to active TB disease, while long-term infection may lead to acquired DNA methylation change. The increased DNA methylation levels of the *LC3B* gene promoter in active TB patients were not reduced after anti-TB treatment. In the in vitro experiment, ESAT-6 stimuli result in significantly increased autophagy flux but non-significant change in DNA methylation level of the *LC3B* gene promoter regions. Thus, we speculate that altered *LC3B* gene methylation is an epigenotype rather than a change in response to *M. tb* infection. Second, increased gene promoter DNA methylation is often associated with decreased expression of the gene. However, DNA methylation change is just one of the mechanisms responsible for gene and protein expression changes. In our cohort, both LC3B expression and DNA methylation levels of the *LC3B* gene promoter were increased in active TB patients, and only the former decreased after anti-TB treatment, while both levels were correlated negatively. We speculate that individuals that carry hypermethylated *LC3B* gene promoter epigenotype may have inadequate autophagy flux at initial confronting with *M. tb* infection and have a higher tendency to progress to active TB disease. Once progression, multiplication of *M. tb* in the human body may induce overt autophagy flux though mechanisms other than DNA methylation change of the ATG genes. Third, DNA methylation levels were determined in PBMC samples but not monocytes, since monocyte isolation often requires a larger amount of blood sample. We could not exclude the possibility that DNA methylation status may behave differently in monocyte and lymphocyte. Fourth, 5-AZA treatment result in improvement in ROS production, late apoptosis, and phagocytosis in the presence of ESAT-6 stimuli, but not in DNA methylation change of the *LC3B* or *ATG5* gene, suggesting that 5-AZA may augment bactericidal, autophagy, apoptosis, and phagocytosis functions of macrophage through demethylating reduction-oxidation or other autophagy-related genes. Finally, Rap treatment at 100/500 nM result in improvement in apoptosis and phagocytosis functions in the presence of ESAT-6 stimuli, but not in DNA methylation change of the *LC3B* or *ATG5* gene. However, a recent study showed that everolimus diminished DNA hypermethylation of genes involved in the PI3K-mTOR, inflammatory, TNF, and IL-6-STAT3 pathways in both macrophage and TB patients [45]. We could not exclude the possibility that Rap at a higher concentration may exert a demethylation effect on the ATG genes.

Conclusions

Increased LC3B (+) percentage of blood M1/2a monocyte, and hypermethylated *LC3B* gene promoter region were independent factors distinguishing active TB disease from either LTBI or NIHS. Combining these ATG-related biomarkers and clinical factors, the Prediction Score 1 and 2 could be calculated to identify patients at risk of progression from either NIHS or LTBI to active TB disease. LC3B and ATG5 expressions were decreased after 6-month anti-TB treatment, but hypermethylated *LC3B* gene promoter region persisted. The in vitro experiments showed that autophagy flux of THP-1 cells was increased in response to ESAT-6 stimuli in association with increased apoptosis, ROS production, and phagocytosis, but DNA methylation levels of the *LC3B* gene promoter region was not altered, while 5-AZA treatment improved these macrophage functions through mechanisms other than demethylation of the *LC3B* or *ATG5* gene promoter region. The findings open the possibility of using ATG-related biomarkers to monitor the progress of *M. tb* infection, and applying a DNA de-methylation agent or epigenetic editing as host-directed therapy in active TB disease.

Abbreviations

M. tb	Mycobacterium tuberculosis
LTBI	Latent TB infection
MAP1LC3; LC3	Microtubule associated protein 1 light chain 3
ROS	Reactive oxygen species
p62	SQSTM1
ATG	Autophagy related genes
NIHS	Non-infected healthy subjects
CpG	Cytosine-phosphate-Guanine
CXR	Chest radiographic
IGRA	Interferon-γ releasing assay
AFB	Acid fast bacilli
MFI	Mean fluorescence intensity
PBMCs	Peripheral blood mononuclear cells
PCR	Polymerase chain reaction
ESAT-6	Early secretory antigenic target-6
5-AZA	5-aza-2′-de-oxycytidine
Rap	Rapamycin
H2DCFDA	2′,7′-dichlorodihydrofluorescein diacetate
PI	Propidium iodide
BMI	Body mass index
AUC	Area under the receiver operating characteristic curves
ROC	Receiver operating characteristic
miR	microRNA

Supplementary Information

The online version contains supplementary material available at https://doi.org/10.1186/s12931-025-03149-1.

Supplementary Material 1

Acknowledgements
The authors acknowledge the technical support provided by the Genomic and Proteomic Core Laboratory, and the Internal Medicine Core Facility of the Kaohsiung Chang Gung Memorial Hospital. The following reagents were obtained through BEI Resources, NIAID, NIH: ESAT-6, Recombinant Protein Reference Standard, NR-49424; Ag85A, Recombinant Protein Reference Standard, NR-49427; ***M. tb*** Strain H37RV, Gamma-Irradiated Whole Cells, NR-49098. Finally, we appreciate the Biostatistics Center, Kaohsiung Chang Gung Memorial Hospital, for statistics work.

Author contributions
MCL and CCH conceived of the study and supervised the project; CCW, TYC, YHW, CCT, and SYL enrolled the participants; CPL, TYW, PYH, and JCC performed the experiments and analyzed the data; YCC and YTF wrote the manuscript.

Funding
This work was supported by grants from the Ministry of Science and Technology, Taiwan (NMRPG8K0081/109-2314-B-182 A-115 and NSTC112-2314-B-182 A-146- to Y.C. Chen) and from Kaohsiung Chang Gung Memorial Hospital (CMRPG8L0311 to Y.C. Chen), Taiwan.

Data availability
All data generated or analyzed during this study are included in this published article and its supplementary information files.

Declarations

Ethics approval and consent to participate
The Chang Gung memorial hospital's institutional review board approved the study protocol (certificate number: 201901817B0), which complies with the Helsinki Declaration. Written informed consent was obtained from all subjects participating in the study, who were aged 20 years or older.

Consent for publication
Not applicable.

Competing interests
The authors declare no competing interests.

Author details
[1]Division of Pulmonary and Critical Care Medicine, Department of Medicine, Kaohsiung Chang Gung Memorial Hospital, Chang Gung University College of Medicine, Kaohsiung 83301, Taiwan
[2]Graduate Institute of Clinical Medical Sciences, Department of Medicine, College of Medicine, Chang Gung University, Taoyuan 33302, Taiwan
[3]Department of Respiratory Therapy, Kaohsiung Chang Gung Memorial Hospital, Chang Gung University College of Medicine, Kaohsiung 83301, Taiwan
[4]Genomics and Proteomics Core Lab, Department of Medical Research, Kaohsiung Chang Gung Memorial Hospital, Kaohsiung 83301, Taiwan

Received: 7 November 2024 / Accepted: 10 February 2025
Published online: 05 March 2025

References

1. Bagcchi S. WHO's Global Tuberculosis Report 2022. Lancet Microbe. 2023;4:e20.
2. Nabity SA, Han E, Lowenthal P, Henry H, Okoye N, Chakrabarty M, Chitnis AS, Kadakia A, Villarino E, Low J, et al. Sociodemographic Characteristics, comorbidities, and Mortality among persons diagnosed with tuberculosis and COVID-19 in close succession in California, 2020. JAMA Netw Open. 2021;4:e2136853.
3. da Costa C, Benn CS, Nyirenda T, Mpabalwani E, Grewal HMS, Ahmed R, Kapata N, Nyasulu PS, Maeurer M, Hui DS, et al. Perspectives on development and advancement of new tuberculosis vaccines. Int J Infect Dis. 2024;141S:106987.
4. Zumla A, Maeurer M. Host-Directed therapies for tackling Multi-drug resistant tuberculosis: learning from the Pasteur-Bechamp debates. Clin Infect Dis. 2015;61:1432–8.
5. Bah A, Vergne I. Macrophage autophagy and bacterial infections. Front Immunol. 2017;8:1483.
6. Sil P, Muse G, Martinez J. A ravenous defense: canonical and non-canonical autophagy in immunity. Curr Opin Immunol. 2018;50:21–31.
7. Paik S, Kim JK, Chung C, Jo EK. Autophagy: a new strategy for host-directed therapy of tuberculosis. Virulence. 2019;10:448–59.
8. Shariq M, Quadir N, Alam A, Zarin S, Sheikh JA, Sharma N, Samal J, Ahmad U, Kumari I, Hasnain SE, Ehtesham NZ. The exploitation of host autophagy and ubiquitin machinery by Mycobacterium tuberculosis in shaping immune responses and host defense during infection. Autophagy. 2023;19:3–23.
9. Sengupta S, Pattanaik KP, Mishra S, Sonawane A. Epigenetic orchestration of host immune defences by Mycobacterium tuberculosis. Microbiol Res. 2023;273:127400.
10. Sudhakar P, Jacomin AC, Hautefort I, Samavedam S, Fatemian K, Ari E, Gul L, Demeter A, Jones E, Korcsmaros T, Nezis IP. Targeted interplay between bacterial pathogens and host autophagy. Autophagy. 2019;15:1620–33.
11. Khalil H, Tazi M, Caution K, Ahmed A, Kanneganti A, Assani K, Kopp B, Marsh C, Dakhlallah D, Amer AO. Aging is associated with hypermethylation of autophagy genes in macrophages. Epigenetics. 2016;11:381–8.
12. Pant R, Kabeer SW, Sharma S, Kumar V, Patra D, Pal D, Tikoo K. Pharmacological inhibition of DNMT1 restores macrophage autophagy and M2 polarization in Western diet-induced nonalcoholic fatty liver disease. J Biol Chem. 2023;299:104779.
13. Shan T, Li LY, Yang JM, Cheng Y. Role and clinical implication of autophagy in COVID-19. Virol J. 2023;20:125.
14. Yang Y, Shu X, Xie C. An overview of Autophagy in Helicobacter pylori infection and related gastric Cancer. Front Cell Infect Microbiol. 2022;12:847716.
15. Wei S, Xu T, Chen Y, Zhou K. Autophagy, cell death, and cytokines in K. pneumoniae infection: therapeutic perspectives. Emerg Microbes Infect. 2023;12:2140607.
16. Silwal P, Paik S, Kim JK, Yoshimori T, Jo EK. Regulatory mechanisms of Autophagy-targeted antimicrobial therapeutics against mycobacterial infection. Front Cell Infect Microbiol. 2021;11:633360.
17. Zhou J, Lv J, Carlson C, Liu H, Wang H, Xu T, Wu F, Song C, Wang X, Wang T, Qian Z. Trained immunity contributes to the prevention of Mycobacterium tuberculosis infection, a novel role of autophagy. Emerg Microbes Infect. 2021;10:578–88.
18. Khan A, Zhang K, Singh VK, Mishra A, Kachroo P, Bing T, Won JH, Mani A, Papanna R, Mann LK, et al. Human M1 macrophages express unique innate immune response genes after mycobacterial infection to defend against tuberculosis. Commun Biol. 2022;5:480.
19. Chen YC, Hsiao CC, Wu CC, Chao TY, Leung SY, Chang YP, Tseng CC, Lee CP, Hsu PY, Wang TY, et al. Next generation sequencing reveals miR-431-3p/miR-1303 as immune-regulating microRNAs for active tuberculosis. J Infect. 2022;85:519–33.
20. Sengupta S, Nayak B, Meuli M, Sander P, Mishra S, Sonawane A. Mycobacterium tuberculosis Phosphoribosyltransferase promotes bacterial survival in macrophages by inducing histone hypermethylation in Autophagy-related genes. Front Cell Infect Microbiol. 2021;11:676456.
21. Chen YC, Hsiao CC, Chen TW, Wu CC, Chao TY, Leung SY, Eng HL, Lee CP, Wang TY, Lin MC. Whole genome DNA methylation analysis of active pulmonary tuberculosis Disease identifies Novel Epigenotypes: PARP9/miR-505/RASGRP4/GNG12 gene methylation and clinical phenotypes. Int J Mol Sci 2020, 21.
22. Caution K, Pan A, Krause K, Badr A, Hamilton K, Vaidya A, Gosu H, Daily K, Estfanous S, Gavrilin MA, et al. Methylomic correlates of autophagy activity in cystic fibrosis. J Cyst Fibros. 2019;18:491–500.
23. Karlsson L, Das J, Nilsson M, Tyren A, Pehrson I, Idh N, Sayyab S, Paues J, Ugarte-Gil C, Mendez-Aranda M, Lerm M. A differential DNA methylome signature of pulmonary immune cells from individuals converting to latent tuberculosis infection. Sci Rep. 2021;11:19418.
24. DiNardo AR, Rajapakshe K, Nishiguchi T, Grimm SL, Mtetwa G, Dlamini Q, Kahari J, Mahapatra S, Kay A, Maphalala G, et al. DNA hypermethylation during tuberculosis dampens host immune responsiveness. J Clin Invest. 2020;130:3113–23.
25. Muhammad JS, Nanjo S, Ando T, Yamashita S, Maekita T, Ushijima T, Tabuchi Y, Sugiyama T. Autophagy impairment by Helicobacter pylori-induced methylation silencing of MAP1LC3Av1 promotes gastric carcinogenesis. Int J Cancer. 2017;140:2272–83.

26. Abd El Maksoud AI, Elebeedy D, Abass NH, Awad AM, Nasr GM, Roshdy T, Khalil H. Methylomic changes of Autophagy-related genes by Legionella Effector Lpg2936 in Infected macrophages. Front Cell Dev Biol. 2019;7:390.
27. Pollock KM, Whitworth HS, Montamat-Sicotte DJ, Grass L, Cooke GS, Kapembwa MS, Kon OM, Sampson RD, Taylor GP, Lalvani A. T-cell immunophenotyping distinguishes active from latent tuberculosis. J Infect Dis. 2013;208:952–68.
28. Hozumi H, Tsujimura K, Yamamura Y, Seto S, Uchijima M, Nagata T, Miwa S, Hayakawa H, Fujisawa T, Hashimoto D, et al. Immunogenicity of dormancy-related antigens in individuals infected with Mycobacterium tuberculosis in Japan. Int J Tuberc Lung Dis. 2013;17:818–24.
29. Agrawal P, Upadhyay A, Kumar A. microRNA as biomarkers in tuberculosis: a new emerging molecular diagnostic solution. Diagn Microbiol Infect Dis. 2024;108:116082.
30. Carranza C, Pedraza-Sanchez S, de Oyarzabal-Mendez E, Torres M. Diagnosis for latent tuberculosis infection: New Alternatives. Front Immunol. 2020;11:2006.
31. Lee S, Lee W, Kang SK. Tuberculosis infection status and risk factors among health workers: an updated systematic review. Ann Occup Environ Med. 2021;33:e17.
32. Dabitao D, Bishai WR. Sex and Gender Differences in Tuberculosis Pathogenesis and treatment outcomes. Curr Top Microbiol Immunol. 2023;441:139–83.
33. Peetluk LS, Ridolfi FM, Rebeiro PF, Liu D, Rolla VC, Sterling TR. Systematic review of prediction models for pulmonary tuberculosis treatment outcomes in adults. BMJ Open. 2021;11:e044687.
34. Cao R, To K, Kachour N, Beever A, Owens J, Sathananthan A, Singh P, Kolloli A, Subbian S, Venketaraman V. Everolimus-induced effector mechanism in macrophages and survivability of Erdman, CDC1551 and HN878 strains of Mycobacterium tuberculosis infection. Biomol Concepts. 2021;12:46–54.
35. Wallis RS, Ginindza S, Beattie T, Arjun N, Likoti M, Edward VA, Rassool M, Ahmed K, Fielding K, Ahidjo BA, et al. Adjunctive host-directed therapies for pulmonary tuberculosis: a prospective, open-label, phase 2, randomised controlled trial. Lancet Respir Med. 2021;9:897–908.
36. Hu X, Zhou X, Yin T, Chen K, Hu Y, Zhu B, Mi K. The mycobacterial DNA methyltransferase HsdM decreases intrinsic Isoniazid susceptibility. Antibiot (Basel) 2021, 10.
37. Rani A, Alam A, Ahmad F, Saurabh PM, Zarin A, Mitra S, Hasnain DK, Ehtesham SE. Mycobacterium tuberculosis Methyltransferase Rv1515c can suppress host defense mechanisms by modulating Immune functions utilizing a multipronged mechanism. Front Mol Biosci. 2022;9:906387.
38. Singh PR, Dadireddy V, Udupa S, Kalladi SM, Shee S, Khosla S, Rajmani RS, Singh A, Ramakumar S, Nagaraja V. The Mycobacterium tuberculosis methyltransferase Rv2067c manipulates host epigenetic programming to promote its own survival. Nat Commun. 2023;14:8497.
39. Singh V, Prakhar P, Rajmani RS, Mahadik K, Borbora SM, Balaji KN. Histone methyltransferase SET8 epigenetically reprograms host Immune responses to assist mycobacterial survival. J Infect Dis. 2017;216:477–88.
40. Prakhar P, Bhatt B, Lohia GK, Shah A, Mukherjee T, Kolthur-Seetharam U, Sundaresan NR, Rajmani RS, Balaji KN. G9a and Sirtuin6 epigenetically modulate host cholesterol accumulation to facilitate mycobacterial survival. PLoS Pathog. 2023;19:e1011731.
41. Yaseen I, Choudhury M, Sritharan M, Khosla S. Histone methyltransferase SUV39H1 participates in host defense by methylating mycobacterial histone-like protein HupB. EMBO J. 2018;37:183–200.
42. Gleneadie HJ, Baker AH, Batis N, Bryant J, Jiang Y, Clokie SJH, Mehanna H, Garcia P, Gendoo DMA, Roberts S, et al. The anti-tumour activity of DNA methylation inhibitor 5-aza-2′-deoxycytidine is enhanced by the common analgesic Paracetamol through induction of oxidative stress. Cancer Lett. 2021;501:172–86.
43. Lin HY, Chuang JH, Wang PW, Lin TK, Wu MT, Hsu WM, Chuang HC. 5-aza-2′-Deoxycytidine Induces a RIG-I-Related Innate Immune Response by Modulating Mitochondria Stress in Neuroblastoma. Cells 2020, 9.
44. Maroufi F, Maali A, Abdollahpour-Alitappeh M, Ahmadi MH, Azad M. CRISPR-mediated modification of DNA methylation pattern in the new era of cancer therapy. Epigenomics. 2020;12:1845–59.
45. Abhimanyu, Longlax SC, Nishiguchi T, Ladki M, Sheikh D, Martinez AL, Mace EM, Grimm SL, Caldwell T, Portillo Varela A, et al. TCA metabolism regulates DNA hypermethylation in LPS and Mycobacterium tuberculosis-induced immune tolerance. Proc Natl Acad Sci U S A. 2024;121:e2404841121.

Publisher's note